

Fiber Bragg Gratings for Dispersion Compensation in Transmission: Theoretical Model and Design Criteria for Nearly Ideal Pulse Recompression

Natalia M. Litchinitser, Benjamin J. Eggleton, and David B. Patterson, *Member, IEEE*

Abstract—We propose a transmission-based dispersion compensator employing an apodized, unchirped fiber Bragg grating (FBG). A theoretical model for dispersion compensation in transmission based on the dispersive properties of the periodic structure is developed. A figure of merit is defined for optimization of the grating parameters for maximum recompression of dispersion-broadened optical pulses in long-haul communication systems. Numerical examples confirm that nearly perfect compensation with very low insertion losses can be achieved for many practical cases of interest.

Index Terms—Compensation, gratings, optical fiber dispersion, optical pulse compression.

I. INTRODUCTION

FIBER gratings are already key components in optical communication links as filters [1], gain flatteners [2], and dispersion compensators [3]. Fiber Bragg gratings (FBG's) are very attractive components because as well as being passive, linear, and compact, they possess strong dispersion in both reflection and transmission. In reflection, the dispersion arises when the edge of the band gap varies with axial position along the grating such as in linearly chirped or ramped gratings [3], [4]. Different wavelengths in a dispersed pulse are reflected at different positions in the grating, leading to different optical path lengths and thus providing the possibility of compensating for dispersion in long-haul fiber links [5], [6]. While the results thus far have been quite impressive, the experiments typically require the use of an optical circulator or 3 dB coupler and the design and fabrication of complex grating structures.

A more attractive solution would be a transmission-based system in which the gratings are placed in line with the fiber. Ouellette [7] studied theoretically the use of uniform Bragg gratings for transmission dispersion compensation and concluded that the maximum achievable compression ratio is severely limited by the small bandwidth of the highly dispersive regions in the transmission spectrum of the grating. Recently there has been renewed interest in using Bragg

gratings in transmission. Dispersion compensation using a uniform fiber Bragg grating in transmission was demonstrated both experimentally and numerically [8], [9]. It was shown that the results of Ouellette's analysis are restricted to the case where the pulse bandwidth is smaller than or comparable to the bandwidths of the sidelobes in the transmission spectrum of the grating. The performance of the transmission-based dispersion compensator was shown to be significantly improved when the pulse bandwidth is much greater than the bandwidths of the sidelobes in the transmission spectrum.

In this paper, we propose a transmission-based dispersion compensator utilizing an apodized, unchirped fiber Bragg grating. We demonstrate that this scheme is a viable alternative to existing dispersion-compensation systems, capable of providing nearly perfect compensation in many practical cases of interest. We derive analytical design equations and define a figure of merit to optimize the grating parameters for maximum pulse recompression.

The paper is structured as follows. In Section II, we analyze the grating performance in terms of the dispersion relation outside the reflection band; here, we replace the grating with a highly dispersive medium. We introduce a figure of merit which allows prediction of the performance of the compensator and grating design for maximum recompression of a dispersion-broadened pulse. Section III discusses the role of apodization on the performance of the dispersion compensator. We show that the oscillations in the transmission spectrum associated with the finite length of the grating can be removed almost entirely using apodization techniques, so that the insertion losses in the compensator can be significantly reduced. In Section IV, we discuss the results of numerical simulations based on coupled-mode equations, demonstrating that almost perfect recompression of dispersed optical pulses can be achieved by using a suitably designed grating. Finally, Section V discusses the limitations of our theoretical model and demonstrates that nearly ideal compensation can always be achieved with sufficiently long, strong gratings, or concatenated gratings.

II. THEORETICAL MODEL

Bragg gratings are known to exhibit strong dispersion in transmission at frequencies close to the edge of the photonic band gap. Here we discuss these dispersion relations and derive design equations for the dispersion compensator, which utilizes the dispersion associated with the band structure of the uniform, unchirped Bragg grating.

Manuscript received February 15, 1997; revised May 5, 1997. The work of N. M. Litchinitser was supported by the Aileen S. Andrew Foundation.

N. M. Litchinitser is with the Electrical and Computer Engineering Department, Illinois Institute of Technology, 3301 S. Dearborn, Chicago, IL 60616 USA. She is now with The Institute of Optics, University of Rochester, Rochester, NY 14627 USA.

B. J. Eggleton is with Department of Optical Physics, Bell Laboratories, Lucent Technologies, Murray Hill, NJ 07974 USA.

D. B. Patterson is with the Electrical and Computer Engineering Department, Illinois Institute of Technology, Chicago, IL 60616 USA.

Publisher Item Identifier S 0733-8724(97)05922-7.

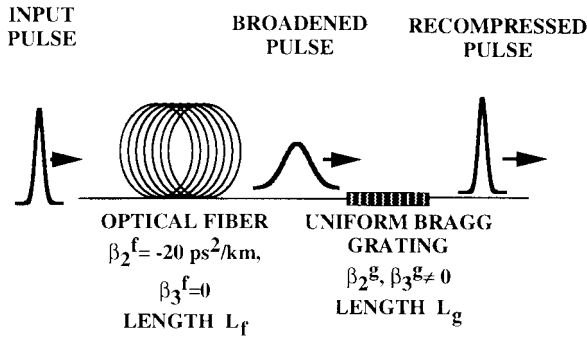


Fig. 1. Schematic diagram of transmission dispersion compensator.

A. Dispersion-Induced Pulse Broadening in Optical Fiber Link

We first consider the problem of optimizing a uniform grating for compression of an initially transform-limited pulse of $1/e$ -width τ_0 , broadened by propagation through optical fiber of length L_f with dispersion β_2^f , as illustrated in Fig. 1. We only consider the second-order fiber dispersion, ignoring higher order fiber dispersion. We also ignore any losses and nonlinear effects in both the fiber and the grating.

A Gaussian pulse maintains its shape with propagation through the fiber, but its width increases due to group-velocity dispersion. The $1/e$ -width τ_f after propagating a distance L_f is related to the initial width τ_0 by the relation [10]

$$\tau_f = \tau_0 \sqrt{1 + \frac{(L_f \beta_2^f)^2}{\tau_0^4}} \quad (1)$$

and the pulse becomes chirped, so that the frequency changes linearly across the pulse with chirp parameter

$$\alpha_f = \frac{L_f}{\beta_2^f \left[L_f^2 + \left(\frac{\tau_0^2}{\beta_2^f} \right)^2 \right]} \quad (2)$$

B. Dispersion Relations for the Grating

We now consider the propagation of this chirped Gaussian pulse in a fiber Bragg grating. In the grating cubic dispersion is significant and cannot be ignored. For now, we ignore finite grating effects, which give rise to sidelobes in the reflection spectrum and oscillations in the delay spectrum. We also ignore fourth and higher order dispersion effects and nonlinear effects of the grating. While this is not exact, we discuss the conditions when this representation is accurate in Sections III and IV.

To describe propagation through a Bragg grating, we need to consider the dispersion relation, which is the relationship between the frequency detuning parameter [11]

$$\delta = \frac{n}{c} (\omega - \omega_B) \quad (3)$$

and the propagation constant $\gamma = \beta - \beta_B$. Here, ω is the optical frequency and ω_B is the resonant Bragg frequency. The dispersion relation is obtained by inserting plane wave solutions into the coupled mode equations, yielding [12]

$$\delta^2 = \gamma^2 + \kappa^2 \quad (4)$$

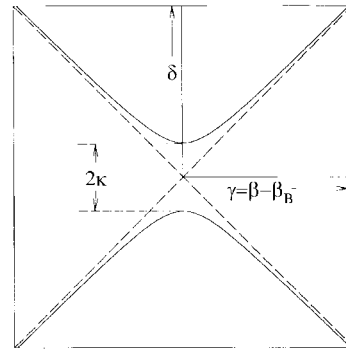


Fig. 2. Photonic band gap for infinite uniform Bragg grating.

where $\kappa = \pi \Delta n \eta / \lambda_B$ is the coupling coefficient, defined by the refractive index modulation, Δn , and the fraction of energy in the core, η . The dispersion curve of (4) is illustrated in Fig. 2, for both a uniform medium (dashed line) and a periodic medium (solid line). Recall that the group velocity dispersion is given by the curvature of the dispersion relation. For the uniform medium the slope is constant, and thus the dispersion is negligible. By introducing a grating, the dispersion relation is modified, with the most noticeable feature being the “photonic band gap” in the dispersion relation: this corresponds to the range of detunings $-\kappa < \delta < \kappa$. For this range of detuning light cannot propagate through the grating and undergoes strong reflection.

Optical pulses detuned outside of the gap ($|\delta| > \kappa$) can propagate, but at velocities that can be substantially less than the speed of light in the uniform medium. The reduced velocity can be understood in terms of the multiple reflections at the grating rulings with a resulting path length increase. The group velocity, $v_g = (c/n) \sqrt{1 - \kappa^2 / \delta^2}$, vanishes at the bandedge and asymptotically approaches c/n far from the Bragg resonance. The range of wavelengths over which this occurs is roughly equal to the bandwidth of the grating; for the fiber gratings we consider in this paper this is of the order of a nanometer. This extreme variation in the group velocity over such a small range of wavelengths leads to strong group velocity dispersion. On the upper branch of the band gap the sign of the dispersion is positive corresponding to anomalous dispersion, where the existence of solitary waves has been experimentally demonstrated [13], [14]. More importantly for this discussion, the normal dispersion exhibited by the grating on the lower side of the photonic band gap can be used to compensate for anomalous dispersion effects caused by fiber propagation at communication wavelengths.

The effects of this grating dispersion can be accounted for mathematically by expanding β in a Taylor series about δ_0 [11]

$$\beta(\delta) = \beta_0^g + \left(\frac{c}{n} \right) \beta_1^g (\delta - \delta_0) + \frac{1}{2} \left(\frac{c}{n} \right)^2 \beta_2^g (\delta - \delta_0)^2 + \frac{1}{6} \left(\frac{c}{n} \right)^3 \beta_3^g (\delta - \delta_0)^3 + \dots \quad (5)$$

where β_n^g is the n th derivative of β with respect to δ evaluated at δ_0 .

We have only included the lowest three terms in this expansion; the accuracy of this relation will be discussed later.

The term $\beta_2^g(\delta)$ is the (quadratic) group velocity dispersion given by

$$\beta_2^g(\delta) = -\left(\frac{n}{c}\right)^2 \frac{\kappa^2}{(\delta^2 - \kappa^2)^{3/2}} \times \text{sign}(\delta) \quad (6)$$

and $\beta_3^g(\delta)$ is the cubic dispersion which is given by

$$\beta_3^g(\delta) = 3\left(\frac{n}{c}\right)^3 \frac{\kappa^2 \delta}{(\delta^2 - \kappa^2)^{5/2}}. \quad (7)$$

Clearly, both β_2^g and β_3^g diverge at the bandedge ($\delta = \kappa$).

In an ideal dispersion compensator, the dispersion of the filter is matched to that of the fiber, i.e.,

$$L_g |\beta_2^g| = L_f |\beta_2^f| \quad (8)$$

where β_2^g is the quadratic dispersion of the grating given by (6) and β_2^f is the quadratic dispersion of the fiber. Here we define an ideal dispersion compensator to be that which recompresses the dispersion-broadened pulse to its transform-limited pulse width. Of course, the cubic dispersion of the grating acts to diminish the efficiency of compression and to distort the pulse, and thus must be as small as possible for the grating to approach ideal behavior.

C. Pulse Propagation in Fiber Bragg Grating

We now model the grating structure by a highly dispersive uniform medium with the quadratic dispersion β_2^g and cubic dispersion β_3^g . This allows us to use the wave equation instead of solving coupled-mode equations to study pulse propagation in the grating. As we neglect fourth and higher order dispersion, the slowly varying amplitude of the pulse envelope satisfies [10]

$$\left(\frac{\partial}{\partial z} + \frac{i\beta_2^g}{2} \frac{\partial^2}{\partial \tau^2} - \frac{\beta_3^g}{6} \frac{\partial^3}{\partial \tau^3}\right) E(z, \tau) = 0 \quad (9)$$

where z is the axial position along the grating.

Following Marcuse [15], [16] and Akhmanov [17], the compression ratio, defined as the ratio of the input to output root mean square (RMS) pulse widths, can be found analytically for the case including quadratic and cubic dispersion

$$C = \left\{ \left(1 - \alpha_f \beta_2^g z\right)^2 + \left(\frac{\beta_2^g z}{\tau_f^2}\right)^2 + \left[1 + (\alpha_f \tau_f^2)^2\right] \left(\frac{\beta_3^g z}{2\tau_f^3}\right)^2 \right\}^{-1/2}. \quad (10)$$

We note that the RMS pulse width gives a good representation of the actual pulse width if the pulse shape is nearly Gaussian, but for non-Gaussian pulses with long, asymmetric leading or trailing edges, the RMS width can be much larger than the full-width at half maximum (FWHM) width. Fixing κ and δ , we find that the compression ratio reaches its maximum at

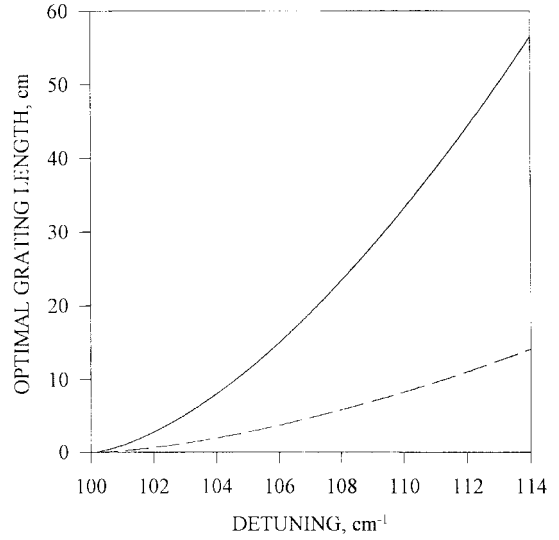


Fig. 3. Optimal grating length as a function of δ for coupling strength $\kappa = 100 \text{ cm}^{-1}$, fiber length $L_f = 400 \text{ km}$ (solid line), and $L_f = 100 \text{ km}$ (dashed line); dispersion $\beta_2^f = -20 \text{ ps}^2/\text{km}$ and $\tau_0 = 24 \text{ ps}$.

$z = L_{\text{opt}}$ along the grating

$$L_{\text{opt}} = \frac{\frac{L_f \beta_2^f}{\beta_2^g}}{1 + \left(\frac{\beta_3^g}{2\beta_2^g \tau_0}\right)^2 \left[\frac{\tau_0^4}{\tau_0^4 + (L_f \beta_2^f)^2}\right]} \quad (11)$$

and equals

$$C_{\text{opt}} = \sqrt{1 + \frac{\left(\frac{L_f \beta_2^f}{\tau_0^2}\right)^2}{1 + \left(\frac{\beta_3^g}{2\beta_2^g \tau_0}\right)^2}}. \quad (12)$$

In Fig. 3, we show the calculated value of L_{opt} from (11) as a function of δ . Note that the optimum length of the grating depends on detuning δ . If now we fix $z = L_g$, then from (1), (2), and (10) the compression ratio varies as

$$C = \left\{ \left(1 - \beta_2^g L_g \alpha_f\right)^2 + \left(\frac{\beta_2^g L_g}{\tau_f^2}\right)^2 + \left[1 + \left(\frac{\beta_3^g}{2\beta_2^g \tau_0}\right)^2\right] \right\}^{-1/2}. \quad (13)$$

D. Figure of Merit

We now introduce a figure of merit, which is useful in analyzing and designing the compensator and represents the relative effects of cubic and quadratic dispersion. Here we analyze the second derivative of the wavenumber β , which represents the group velocity dispersion. Differentiating the Taylor expansion for $\beta(\delta)$ in (5) one arrives at

$$\beta_2(\delta) = \beta_2^g + \frac{c}{n} \beta_3^g (\delta - \delta_0) + \frac{1}{2!} \left(\frac{c}{n}\right)^2 \beta_4^g (\delta - \delta_0)^2 + \frac{1}{3!} \left(\frac{c}{n}\right)^3 \beta_5^g (\delta - \delta_0)^3 + \dots \quad (14)$$

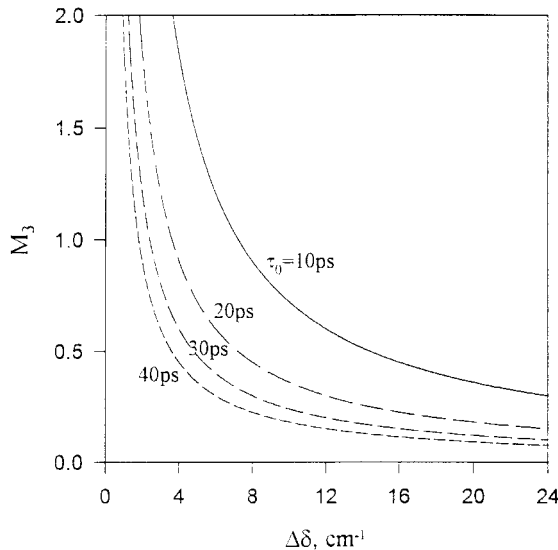


Fig. 4. The calculated value of M_3 as a function of $\Delta\delta$ for pulse widths of $\tau = 10$ ps (solid line), $\tau = 20$ ps (long dashed line), $\tau = 30$ ps (dashed line), and $\tau = 40$ ps (short dashed line).

Then we define a figure of merit as a the ratio between the third- and second-order dispersion terms in this expansion

$$M_3 = \frac{\beta_3^g}{\beta_2^g \tau_0} = \frac{n}{c\tau_0} \frac{3\delta}{\delta^2 - \kappa^2}. \quad (15)$$

Clearly, for optimum pulse compression the third-order dispersion must be small, and thus we desire M_3 to be as small as possible, i.e., $M_3 \ll 1$.

For convenience, we now define the detuning offset, $\Delta\delta = |\delta - \kappa|$, i.e., the detuning with respect to the edge of the photonic band gap. Then M_3 can be written as

$$M_3 = \frac{3n}{\tau_0 c} \frac{\Delta\delta + \kappa}{\Delta\delta^2 + 2\Delta\delta\kappa}. \quad (16)$$

We note that when $\Delta\delta \ll \kappa$, (16) can be approximated by

$$M_3 = \frac{\beta_3^g}{\beta_2^g \tau_0} \approx \frac{3n}{2\tau_0 c} \frac{1}{\Delta\delta}. \quad (17)$$

Fig. 4 shows the calculated value of this approximate M_3 as a function of $\Delta\delta$ for pulse widths of $\tau_{\text{FWHM}} = 10$ ps (solid line), $\tau_{\text{FWHM}} = 20$ ps (long dashed line), $\tau_{\text{FWHM}} = 30$ ps (dashed line), and $\tau_{\text{FWHM}} = 40$ ps (short dashed line). At detunings close to the band gap edge M_3 diverges.

Fig. 5 shows M_3 as a function of the detuning offset $\Delta\delta$ for $\tau_0 = 24$ ps. The range of detuning is divided into three regions for which the dispersion compensator behavior differs. Region I corresponds to the range of detunings in which the spectral half-width of the transform-limited pulse is greater than the detuning offset $\Delta\delta$. In this region, characterized by $\Delta\delta < n/(c\tau_0)$, two effects lead to nonideal recompression. First, reflection of spectral components in the gap reduces pulse energy and may be misinterpreted as compression. Second, higher order dispersion terms dominate near the edge, making

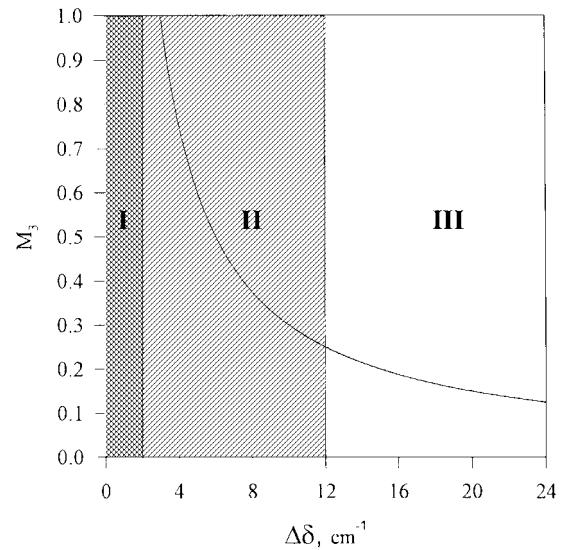


Fig. 5. The approximate value of M_3 as a function of $\Delta\delta$ for transform-limited pulse width $\tau_0 = 24$ ps.

our approximations invalid in this region. We shall discuss these dispersion effects further in Section V.

In Regions II and III, the reflection is no longer present; however, Region II still exhibits appreciable third-order, as well as higher order, dispersion effects which cause nonideal recompression. The third-order dispersion limitation is clearly illustrated in Fig. 6, where we plot the optimal compression ratio (in our third-order approximation) versus M_3 for a pulse which has been broadened by a factor of 3.62 via propagation through a dispersive fiber. For this figure, we have used (12) and (17) to express the optimal compression versus M_3

$$C_{\text{opt}} = \sqrt{1 + \frac{\left(\frac{L_f \beta_2^f}{\tau_0^2}\right)^2}{1 + \left(\frac{M_3}{2}\right)^2}}. \quad (18)$$

From Fig. 6, we observe that for $M_3 > 0.25$ the optimal compression decreases rapidly from the ideal transform-limited value (3.62), indicating that higher order dispersion effects are present despite satisfying the condition $M_3 < 1$. However, in Region III, where $M_3 < 0.25$, the compression approaches this value. In Sections IV and V, we shall also demonstrate, through numerical examples, that under the condition $M_3 < 0.25$ the theory presented in this section is accurate and nearly ideal compensation is achievable. Thus, we define the condition $M_3 < 0.25$ to be a goal for the design of transmission-based compensators.

We now determine the optimal detuning offset for maximum pulse recompression under the approximation $\Delta\delta \ll \kappa$. Rearranging (17), one finds

$$\Delta\delta \approx \frac{3n}{2\tau_0 c} \frac{1}{M_3}. \quad (19)$$

The grating quadratic dispersion, (6), in terms of $\Delta\delta$ is

$$\beta_2^g = -\left(\frac{n}{c}\right)^2 \frac{\kappa^2}{(\Delta\delta^2 + 2\kappa\Delta\delta)^{3/2}} \quad (20)$$

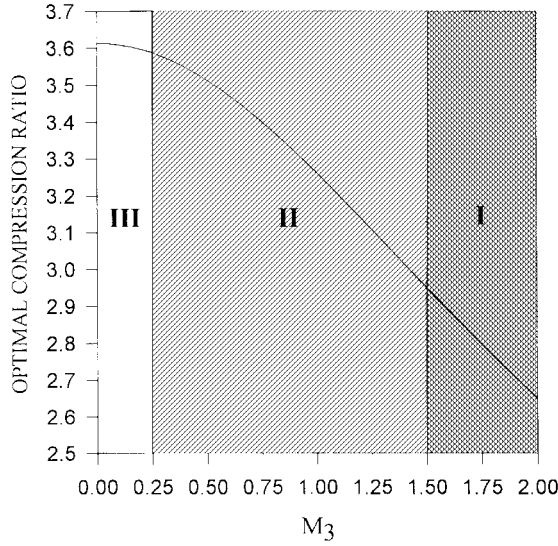


Fig. 6. The optimal compression ratio versus M_3 for $L_f = 100$ km and $\tau_0 = 24$ ps.

which is plotted in Fig. 7 as a function of κ for $\Delta\delta = 5$ cm^{-1} (solid line), $\Delta\delta = 10$ cm^{-1} (short dashed line), $\Delta\delta = 15$ cm^{-1} (long dashed line), and $\Delta\delta = 20$ cm^{-1} (dotted line). Fig. 7 illustrates that strong gratings are required for compensating large dispersion and that the quadratic dispersion, β_2^g , increases close to the edge of the photonic band gap. In the limit that $\Delta\delta \ll \kappa$, (20) can be approximated by

$$\beta_2^g \approx -\left(\frac{n}{c}\right)^2 \frac{\kappa^{1/2}}{(2\Delta\delta)^{3/2}}. \quad (21)$$

By rearranging (21) and using (8) one arrives at

$$\Delta\delta = \frac{1}{2} \left(\frac{n}{c}\right)^{4/3} \kappa^{1/3} \left(\frac{L_g}{\beta_2^f L_f}\right)^{2/3} \quad (22)$$

which shows the detuning for maximum recompression of the dispersed pulse, under the approximation $\Delta\delta \ll \kappa$. The exact value of the optimum central detuning of the incident pulse can be obtained by combining (6) and (8) to yield

$$\delta^6 - 3\delta^4 \kappa^2 + 3\kappa^4 \delta^2 - \kappa^6 - \left(\frac{n}{c}\right)^4 \left(\frac{L_g}{L_f \beta_2^f}\right)^2 \kappa^4 = 0 \quad (23)$$

the positive real root of which represents the optimum detuning for dispersion compensation. However, (22) is accurate for most cases of interest. It also follows from (17) and (22) that M_3 can be well approximated by

$$M_3 \approx \frac{3}{\tau_0} \left(\frac{n}{c}\right)^{-1/3} |\beta_2^f|^{2/3} \cdot \left(\frac{L_f}{L_g}\right)^{2/3} \kappa^{-1/3}. \quad (24)$$

Finally, we note that these approximate equations for $\Delta\delta \ll \kappa$ agree well with third-order dispersion theory. These design equations will provide optimum compensation only under conditions where M_3 is kept small. In Section V, we show that (24) can be used to scale the grating parameters for given fiber length L_f .

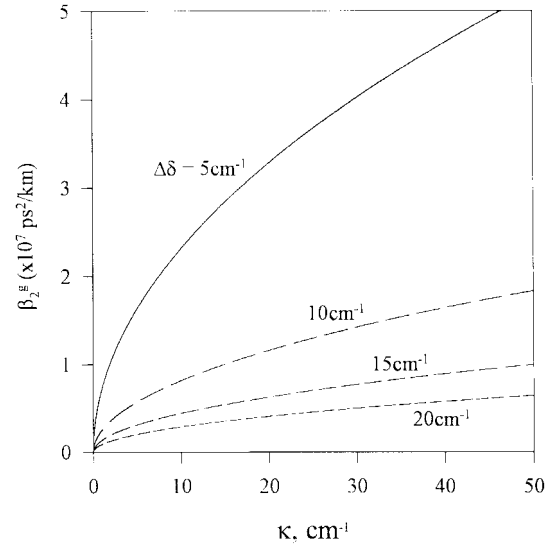


Fig. 7. The calculated value of β_2^g as a function of κ for $\Delta\delta = 5$ cm^{-1} (solid line), $\Delta\delta = 10$ cm^{-1} (long dashed line), $\Delta\delta = 15$ cm^{-1} (dashed line), and $\Delta\delta = 20$ cm^{-1} (short dashed line).

III. FINITE GRATING EFFECTS

In Section II, we considered propagation in an infinite grating. Here we discuss transmission through a finite uniform grating. In particular, we consider the role of the oscillations in the dispersion spectrum of such a grating. This can be best understood if we consider Fig. 8(a) which shows the calculated delay for a uniform grating with $\kappa = 5$ cm^{-1} and length $L_g = 1$ cm. It is calculated using the standard equation

$$T_{\text{delay}} = \frac{\partial\phi}{\partial\omega} \quad (25)$$

where ϕ is the phase of the complex reflectivity which can be found in closed form. The results of (25), though providing an exact rather than approximate solution, must be interpreted carefully.

First, note that at detunings far from the Bragg resonance the group delay in transmission is 50 ps which is, the time taken for light to travel through 1 cm of uniform medium. At detunings closer to the edge of the band gap where the grating is mostly transmitting, the delay oscillates rapidly. These oscillations in the delay spectrum are associated with reflections from the ends of the grating, giving rise to low finesse Fabry–Perot-like resonances [12]. The increased delay can be attributed to the path length increase caused by multiple reflections in the Fabry–Perot cavity. The dashed line shows the calculated delay ignoring end effects.

Now consider the case when the pulse bandwidth is larger than the resonance spacing. The effect of the fluctuations may be easiest to consider using the transform relations between the frequency and time domain. The rapid oscillations in the frequency domain may be considered to be energy that is located at large time delays, i.e., it is “pushed” out of the main pulse. The slowly varying part of the spectrum, found by smoothing or averaging over these ripples, represents the grating effect on the frequency components within the main pulse. Thus, if the energy in the fast oscillations is small

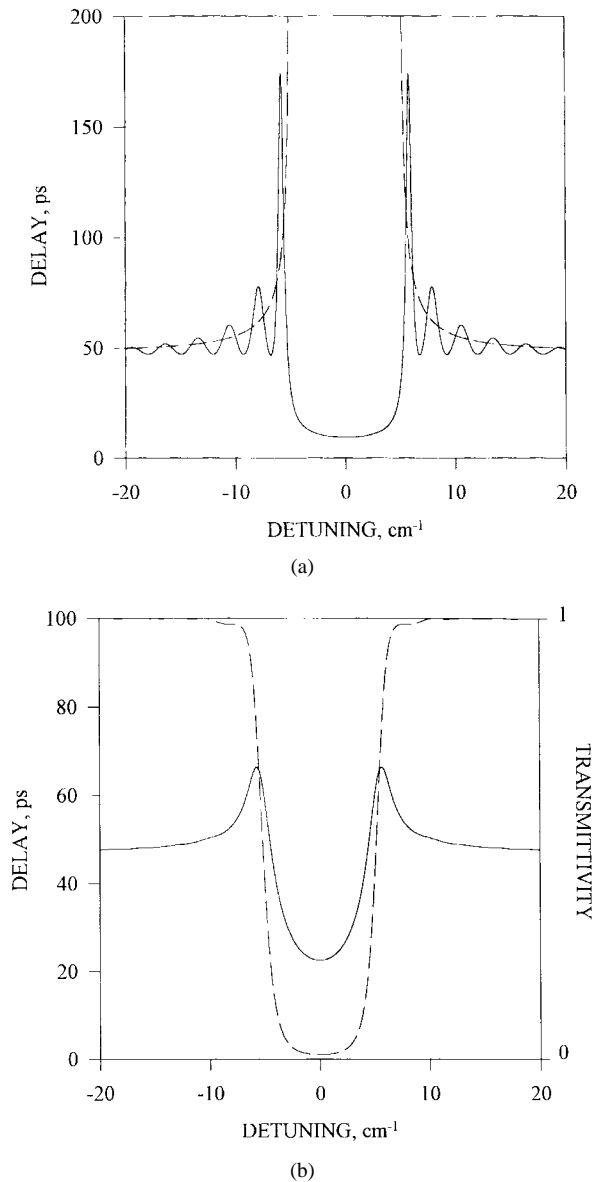


Fig. 8. (a) The calculated group delay for a uniform grating ($L_g = 1$ cm and $\kappa = 5$ cm⁻¹) in transmission (solid line) and the delay in transmission (dashed line), ignoring end effects. (b) The calculated the delay in transmission (solid line) for an apodized grating ($L_g = 1$ cm and $\kappa = 5$ cm⁻¹) and transmission spectrum (dashed line).

compared to the total energy, we may effectively average these out to expose the underlying dispersion relation of the infinite grating. The spacing of the oscillations for a uniform grating of length 1 cm with $\kappa = 5$ cm⁻¹ is approximately 0.01 nm, while the bandwidth of typical pulses is of the order of 0.1 nm. In the time domain this is equivalent to saying that the length of the pulse is shorter than the length of the grating. In this regime interference effects do not occur, thus rendering the oscillations shown in Fig. 7 unimportant. Of course, if the bandwidth of the pulse is smaller than or comparable to the spacing of the oscillations, then the interference effects become important, and thus Ouellette's analysis [7] may be used to show that negligible compression is expected.

While the oscillations in the delay may not be detrimental in terms of the compression they do result in out of band

reflections which reduce the peak intensity of the transmitted pulse. Apodization is a well-known technique which effectively removes the sidelobes in the reflection spectrum of a uniform grating by allowing the index modulation to vanish smoothly at each end [18]. This largely removes the Fabry-Perot reflections which occur at the boundary between the grating and the surrounding medium, thus suppressing the sidelobes and the oscillations in the delay spectrum. The transmission spectrum corresponding to an apodized grating of length 1 cm is shown in Fig. 8(b). The region of the grating in which the coupling coefficient is constant is 0.5 cm ($\kappa = 5$ cm⁻¹). The delay for this apodized grating, shown in Fig. 8(b), is similar to that shown by the dashed line in Fig. 8(a). More importantly, however, is that the grating reflection is negligible at detunings outside the photonic band gap.

IV. NUMERICAL RESULTS

We now combine the results obtained in the previous sections to study the dispersion compensation numerically for three practical examples. This allows us to consider actual finite uniform or nonuniform grating effects, avoiding any approximations and, therefore, to predict where the theory derived in Section II is accurate. Here we use a fundamental matrix approach [19] to solve the coupled-mode equations for nonuniform gratings.

Example I: As a first example we consider a uniform grating with $\kappa = 50$ cm⁻¹ and length $L_g = 10$ cm, for compensating dispersion in a fiber link of length $L_f = 100$ km. We consider a pulse with $\tau_{FWHM} = 40$ ps at 1.55 μ m where the dispersion is $\beta_2^f = -20$ ps²/km. Solving (22) numerically gives an optimum detuning offset of $\Delta\delta = 9.09$ cm⁻¹, corresponding to Region II in Fig. 6. Note that $\Delta\delta \ll \kappa$ so that the approximation leading to (17) is justified, with $M_3 \approx 0.33$. This suggests that, although quadratic dispersion dominates cubic dispersion, the higher order effects are not negligible in this case.

We now model the grating characteristics numerically. Shown in Fig. 9 are the results of recompression via transmission through the grating described above. The transform-limited pulse is broadened to 144 ps (FWHM) upon propagation through the dispersive fiber and compressed back to approximately 46 ps upon transmission through the 10-cm-long grating. The pulse is retarded in time by approximately 900 ps, indicating that the pulse propagates along the length of the grating at an average velocity of 53% of the speed of light in the uniform medium. The reduced peak intensity is associated with out of band reflections and residual cubic dispersion; note that the peak intensity of the compressed pulse is approximately 40% of the transform-limited pulse.

Fig. 10(a) and (b) shows, respectively, the compression ratio and peak intensity versus the central detuning of the initial pulse. Note that the compression ratio peaks at $\delta_{opt} \approx 59.09$ cm⁻¹, consistent with our analytical results. For detunings $\delta < \delta_{opt}$ close to the band gap, dispersion orders higher than two become large and reduce the efficiency of compression. For detunings $\delta > \delta_{opt}$ the group velocity dispersion β_2^g is too

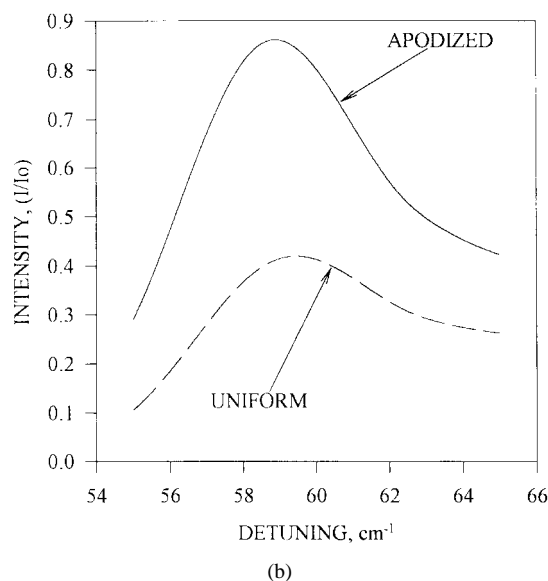
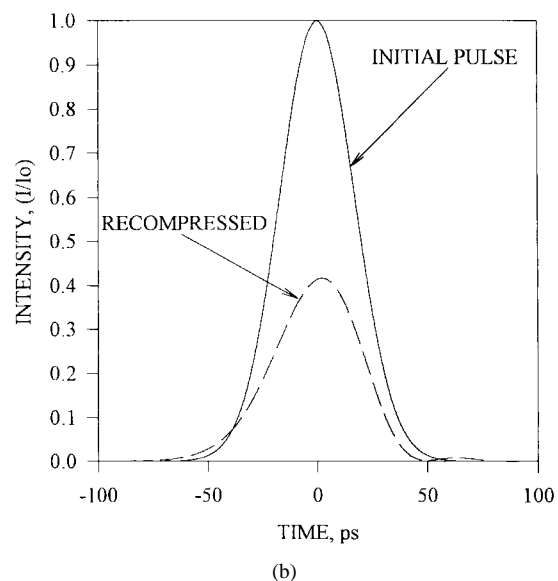
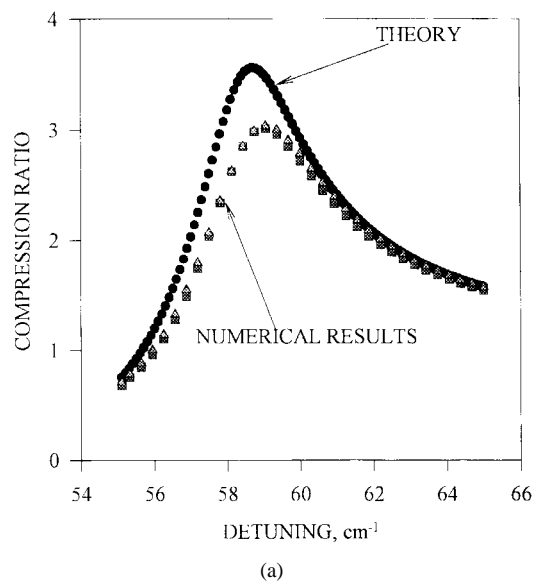
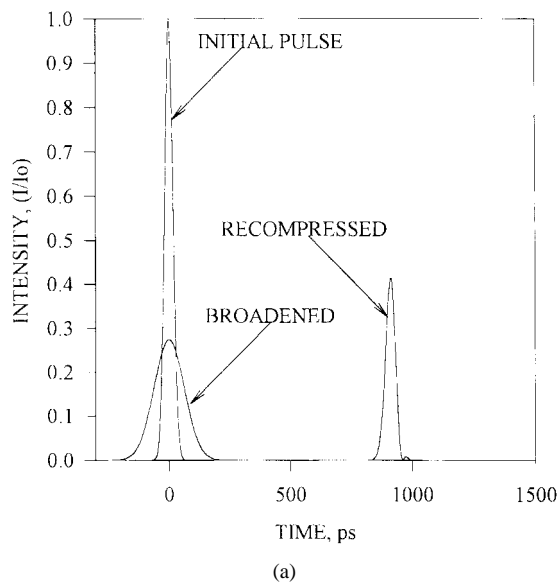


Fig. 9. (a) Initial, broadened and recompressed pulses after transmission through 100 km of fiber and 10 cm uniform grating with $\kappa = 50 \text{ cm}^{-1}$ and $\Delta\delta = 9.09 \text{ cm}^{-1}$ and (b) recompressed pulse superimposed on transform limited pulse.

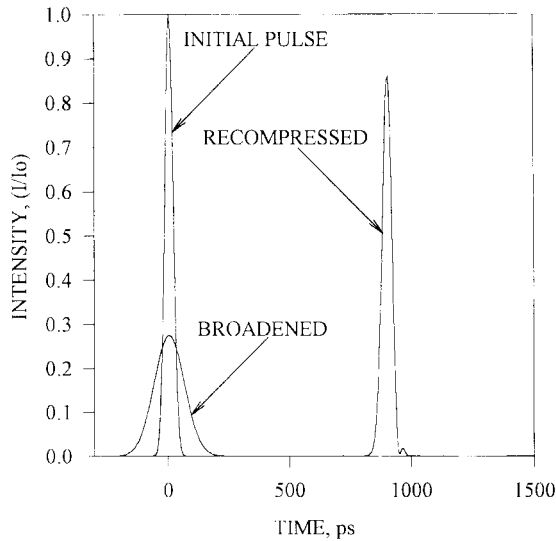
Fig. 10. (a) The compression ratio as a function of δ for a 40-ps pulse broadened to 144 ps by propagation through 100 km of fiber and recompressed via transmission through a 10-cm long uniform (triangles) and apodized (squares) grating with $\kappa_0 = 50 \text{ cm}^{-1}$, compared with theoretical curve (circles). (b) The peak intensity of recompressed pulse normalized to the intensity of initial transform-limited pulse as a function of δ .

small, so that the grating length must be increased (for fixed κ) to satisfy condition (8). Of interest is that the bandwidth corresponding to compression ratios which are greater than two is 5 cm^{-1} . The bandwidth can always be improved by either making the grating longer or stronger.

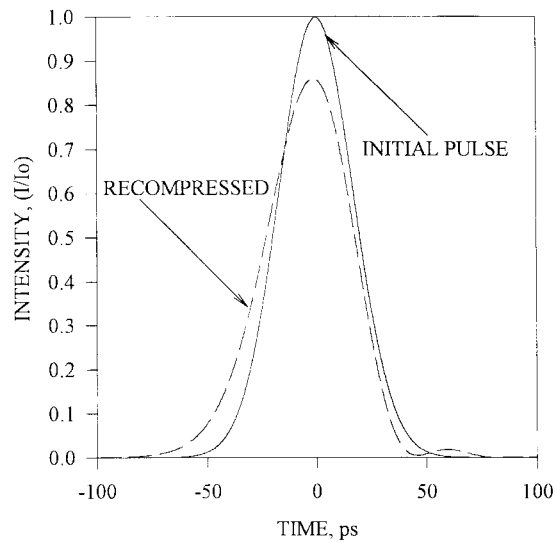
We next suitably apodize the grating such that the coupling coefficient vanishes smoothly at each end of the grating, with a form shown in (26) at the bottom of the page where $\kappa_0 = 50 \text{ cm}^{-1}$, $L_1 = 4.75 \text{ cm}$, $L_2 = 5 \text{ cm}$, and $\Delta L = 0.125 \text{ cm}$.

The compression ratio and peak intensity versus the central detuning of the initial pulse are also shown in Fig. 10(a) and (b). We compare those optimization curves with the theoretical one obtained from (13), observing that compression is relatively unchanged with apodization, while intensity transmission is improved by a factor greater than two over the uniform grating.

$$\kappa(z) = \begin{cases} \kappa_0 & |z| \leq L_1 \\ \kappa_0 \exp \left[-\frac{(z - L_1)^2}{(\Delta L)^2} \right] & L_1 \leq z \leq L_2, -L_2 \leq z \leq -L_1 \\ 0 & |z| \geq L_2 \end{cases} \quad (26)$$



(a)



(b)

Fig. 11. (a) Initial, broadened and recompressed pulses after transmission through 100 km of fiber and 10-cm long apodized grating with $\kappa = 50 \text{ cm}^{-1}$ and $\Delta\delta = 9.09 \text{ cm}^{-1}$ and (b) recompressed pulse superimposed on transform limited pulse.

The results of recompression via transmission through the apodized grating are shown in Fig. 11. We note that only around 1% of the energy is reflected from the grating and that the pulse is recompressed to 49 ps, nearly the transform limited width. Note that the peak intensity is now approximately 85% of the initial peak intensity, representing an insertion loss of 0.7 dB.

Example II: Now we consider the same fiber system as in Example I ($\tau_0^{\text{FWHM}} = 40 \text{ ps}$, $\tau_f^{\text{FWHM}} = 144 \text{ ps}$, $L_f = 100 \text{ km}$), but increase the grating parameters to $\kappa = 100 \text{ cm}^{-1}$ and $L_g = 20 \text{ cm}$. (Such strong gratings have been fabricated in laboratories, exhibiting index modulations as large as 10^{-2} [20]). For this grating, the calculated value of $M_3 = 0.17$, corresponds to Region III in Fig. 6 where nearly perfect compensation can be expected. This near-ideal behavior is demonstrated in Fig. 12, where we plot the ratio of the

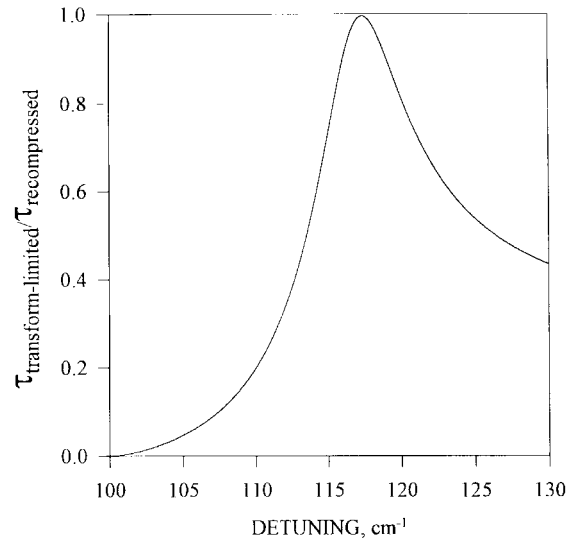


Fig. 12. The ratio of the transform-limited pulse width to the recompressed pulse width for Example II.

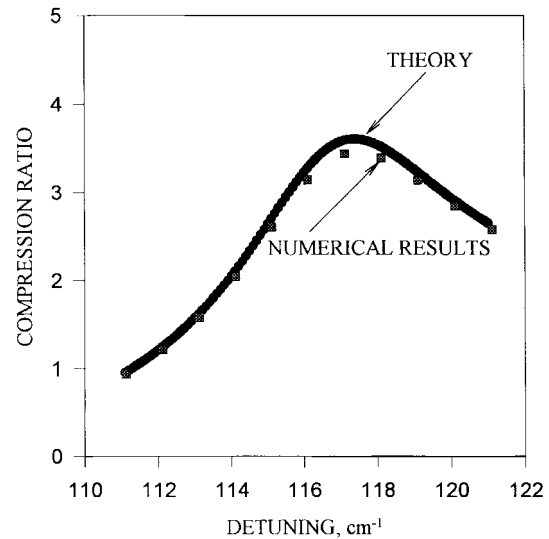


Fig. 13. Compression ratio versus δ for Example II: numerical results (squares) and theoretical values (circles).

transform-limited pulse width to the recompressed pulse width predicted theoretically for this case. Here, we observe that the ratio approaches unity at the optimum detuning, $\delta = 117.37 \text{ cm}^{-1}$.

Fig. 13 compares the theoretical and numerical results for the compression ratio. Here we note that the bandwidth corresponding to compression ratios which are greater than two is approximately 1.6 times greater than that for the weaker, shorter grating of Example I. If we now apodize this 20-cm-long grating ($\kappa = 100 \text{ cm}^{-1}$), we find that the peak intensity increases to 95% of the initial peak intensity, so that the insertion losses in the system are less than 0.25 dB. This indicates that almost perfect recompression can be obtained using longer and stronger apodized gratings in transmission.

Example III: We now consider an example more typical of future long-haul fiber communication systems where the repeater spans are expected to be 400 km. The 40 ps (FWHM)

transform-limited pulse is broadened to 557 ps (FWHM) upon propagation through a 400-km dispersive fiber. Now we can scale the grating parameters in order to maintain the small figure of merit M_3 . We note that the grating parameters can be scaled for any fiber length L_f using (24) in order to obtain $M_3 \ll 1$. Of course, we are limited by the refractive index modulation depth and grating lengths that are available. In this example, we again use a 20-cm-apodized grating with an apodization function of the form of (26), with $L_1 = 9.5$ cm, $L_2 = 10$ cm, $\Delta L = 0.25$ cm, and $\kappa_0 = 100$ cm $^{-1}$.

Fig. 14(a) and (b) shows the compression ratio and peak intensity versus the central detuning of the initial pulse. The transmitted pulse corresponding to $\delta = 107.23$ cm $^{-1}$ is shown in Fig. 15. Though the compression ratio in terms of RMS width for this pulse is only 4.3, the FWHM compression is 8.7. The latter corresponds to a 64-ps pulse width if we ignore the structure at the trailing edge of the pulse. We discuss these results in more detail in the next section, but here we simply note that it is misleading to use the FWHM definition for the detunings $\delta \leq 107.23$ cm $^{-1}$ (δ_{opt}) where higher order dispersion and edge effects dominate and produce highly asymmetric pulse shapes.

V. DISCUSSION

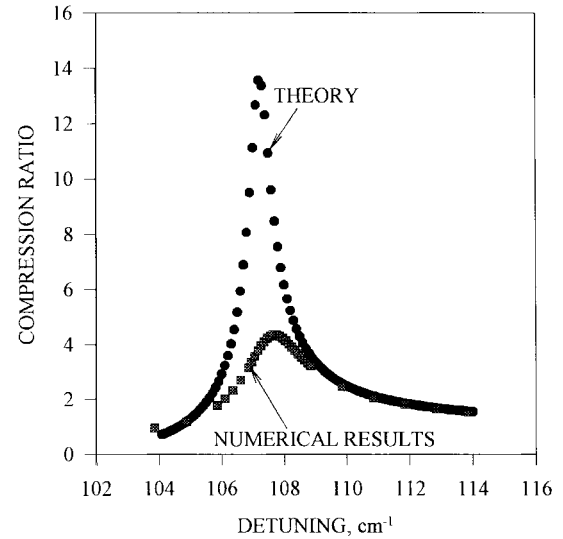
We now discuss the limitations of our analytical analysis. Numerical Examples I and II confirm that this model is accurate for the case of a relatively strong grating used to compensate for dispersion in a fiber length of 100 km. We showed that apodization largely removes the sidelobes in the transmission spectrum of a uniform grating and allows one to achieve almost perfect recompression of dispersed optical pulses, in terms of both pulse width and peak intensity.

Next, we compare and discuss the theoretical and numerical results obtained in the third example where a 20-cm long grating was used for dispersion compensation in a 400-km-long fiber. As we showed there, our numerical results for compression ratio in terms of RMS pulse width and FWHM disagree by a factor of two at the optimal detuning of the pulse central frequency. We note that for a non-Gaussian pulse, the pulse width is not well defined and the RMS value does not give a good representation of the actual pulse width. However, even the compression ratio obtained based on the more liberal FWHM measure is only 64% of the theoretically predicted ratio, indicating the presence of dispersion effects higher than third order.

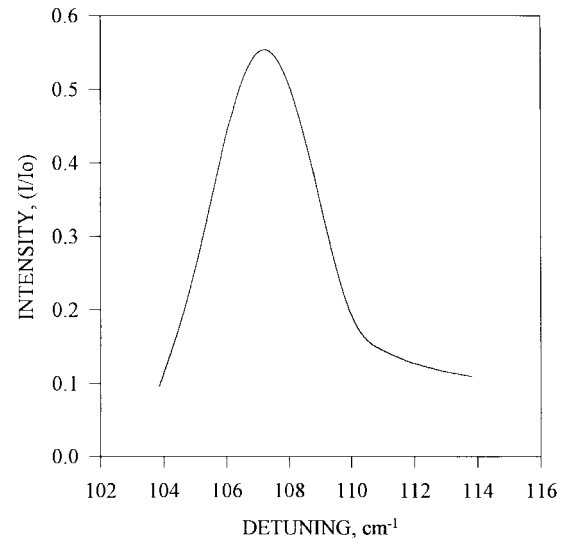
To predict where the fourth and higher order dispersion terms may become important, we again analyze the second derivative of the wavenumber β given by (14). We define the parameters M_n as $\beta_n^q / [(n-2)\beta_{n-1}^q \tau_0]$ similar to the definition of M_3 in (15) and plot them as functions of δ for $n = 3, 4$ (Fig. 16).

Then M_4 is given, in exact and approximate ($\Delta\delta \ll \kappa$) form

$$M_4 = \frac{n}{2t_0c} \frac{\kappa^2 + 4\delta^2}{\delta(\delta^2 - \kappa^2)} \approx \frac{5n}{4\tau_0c\Delta\delta}. \quad (27)$$



(a)



(b)

Fig. 14. (a) The compression ratio versus δ for Example III: numerical results (squares) and theoretical values (circles). (b) The peak intensity of the recompressed pulse (normalized to the intensity of initial transform-limited pulse) versus δ .

Obviously to minimize the effect of the third and higher order terms in (14), we desire all M_n to be as small as possible, i.e., $M_n \ll 1$. If we now calculate M_n for our examples at δ_{opt} , we arrive at the following values for (M_3, M_4) : Example I: (0.33, 0.28); Example II: (0.17, 0.14); and Example III: (0.42, 0.35). Our results indicate that both FWHM and RMS measures agree with the theoretical curve for $M_4 < 0.2$, corresponding in our examples to $\Delta\delta \geq 12$ cm $^{-1}$, as illustrated in Fig. 16. Using this condition for M_4 and (27), we obtain an empirical the condition on $\Delta\delta$ for which fourth-order dispersion effects may be neglected: $\Delta\delta \geq 25n/4c\tau_0$. If, for given grating strength κ , one selects δ_{opt} above this threshold, the dispersion compensator performance will be close to ideal, as described by (9). The corresponding optimal grating length L_g can be obtained from (11) or Fig. 3.

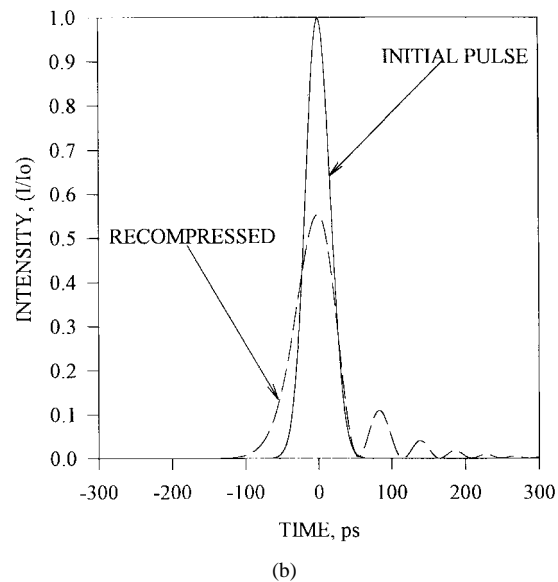
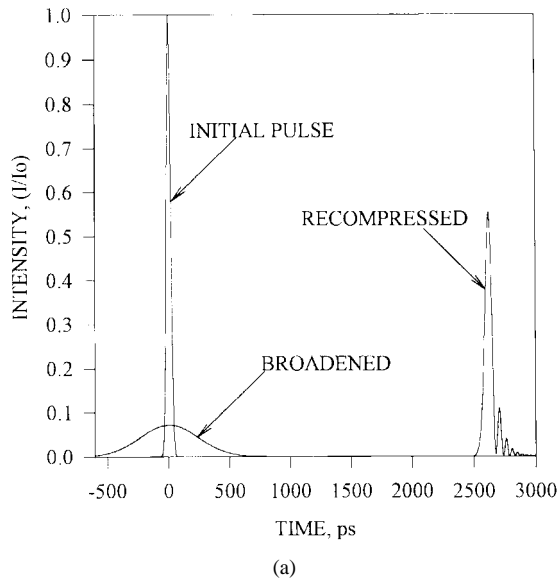


Fig. 15. (a) Initial, broadened and recompressed pulses after transmission through 400 km of fiber and 20 cm long apodized grating with $\kappa = 100 \text{ cm}^{-1}$ and $\Delta\delta = 7.23 \text{ cm}^{-1}$ and (b) recompressed pulse superimposed on transform limited pulse.

Fig. 16 shows that for $\Delta\delta \leq 12 \text{ cm}^{-1}$ higher order dispersion terms become as significant as the third-order term. Therefore higher order terms ($n > 3$) in the Taylor expansion of (5) should be taken into account to predict the grating performance. This explains the disagreement of the numerical results in Fig. 14(a) with the theoretical curves for the parameters of Example III ($\Delta\delta = 7.23 \text{ cm}^{-1}$). While the analysis we have presented can be extended to treat the case of higher order dispersion [21], this is beyond the scope of this paper, and the numerical solution is just as simple to implement as the generalized theory. However, we note that (21) provides accurate design parameters, and the plots of the parameters M_n give a qualitative insight into the physics of the device.

It is worth discussing the results of Examples I and II in Section IV in terms of M_n ($n > 2$). In these examples, $\Delta\delta$ was

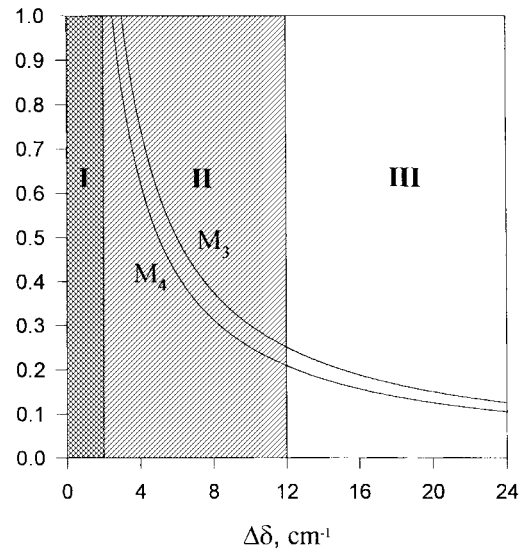


Fig. 16. The calculated values of M_3 and M_4 versus $\Delta\delta$ for $\tau_0 = 24 \text{ ps}$.

9.09 and 17.37 cm^{-1} , respectively; from Fig. 16 we observe that though quartic and higher order dispersion are not negligible in the first example, their relative effect is less than for the third example. Example II clearly illustrates that by making gratings longer and stronger almost perfect recompression can be obtained. In practice, of course, the design parameters are restricted by the refractive index changes and grating lengths that are available.

VI. CONCLUSIONS

We have proposed the use of apodized, unchirped fiber Bragg gratings for dispersion compensation in transmission. The problem of optimizing a grating structure for maximum recompression of a dispersed pulse was analyzed using the third-order approximation of dispersion theory. We discussed the limitation of our analysis and considered three numerical examples which demonstrated that by making gratings longer or stronger, we can keep the figure of merit M_3 small. In this case, the third-order dispersion effects are negligible, and almost perfect recompression of dispersed optical pulses can be achieved. We showed that apodization effectively suppresses the oscillations in the delay spectrum and the sidelobes in the uniform grating spectrum so that the insertion losses at the grating output could be reduced to less than 0.25 dB.

It is worth comparing the transmission dispersion compensator to reflection-based dispersion compensators. The chirped grating which has attracted so much attention clearly has the advantages of both larger bandwidth and larger dispersion. These properties make it attractive for use in a dispersion compensation link. However, the component suffers from the disadvantages of requiring complicated designs and requiring either a circulator or a 3 dB coupler. A transmission-based dispersion compensator, as presented here, does have a limitation in bandwidth imposed by the grating parameters. However, we note that the performance of the transmission dispersion compensator can always be improved by either making the

grating longer or stronger. This allows not only improvement in the compression ratio but also an increase in the bandwidth over which this compression can be achieved. These devices will also impart lower insertion losses than reflective designs, as they may be spliced in-line with the fiber link.

In addition, these devices could be used in wavelength-division multiplexing (WDM) applications [22], [23] if multiple compensators were used in a system with channel spacing much greater than the grating band gaps. Our results may be useful in other grating-based wavelength selective applications such as add/drop filters [24], where apodized gratings can be utilized to reduce the reflection outside the band gap. Care should be taken to ensure that the grating produces no dispersion broadening on adjacent channels. Therefore, those WDM systems should be designed so that each channel is truly noninteracting.

In this paper, we considered dispersion compensation in transmission based only on the dispersion associated with the band structure of the grating. In principle, the grating dispersion can be tailored by using nonuniform grating designs or by grating concatenation. In particular, dispersion compensation using a ramped fiber Bragg grating in transmission was demonstrated experimentally [8]. However the grating was not optimized for maximum compression. Another possibility is the use of superstructure Bragg gratings [25] which could possibly relax the constraints on grating parameters and give an additional degree of freedom in the design.

In summary, we have proposed an attractive alternative to existing dispersion-compensation schemes. The component has applications in both digital telecommunications and analog transmission systems, where the losses incurred in chirped grating/circulator schemes or in kilometers of dispersion-compensating fiber are detrimental to system performance. The low loss of our system, combined with nearly perfect recompression, should make these transmission-based compensators a viable solution in many of these applications.

ACKNOWLEDGMENT

The authors would like to acknowledge fruitful conversations with Dr. P. A. Krug, Dr. C. Martijn de Sterke, Dr. R. E. Slusher, Dr. V. A. Vysloukh, and Dr. Thomas A. Strasser.

REFERENCES

- [1] G. Meltz, W. W. Morey, and W. H. Glenn, *Opt. Lett.*, vol. 14, p. 823, 1989.
- [2] A. M. Vengsarkar, J. R. Pedrazzani, J. B. Judkins, and P. J. Lemaire, *Opt. Lett.*, vol. 21, p. 336, 1996.
- [3] F. Ouellette, *Opt. Lett.*, vol. 12, p. 847, 1987.
- [4] T. Stephens, P. A. Krug, Z. Brodzeli, G. Dhosi, F. Ouellette, and L. Poladian, *Electron. Lett.*, vol. 32, p. 1599, 1996.
- [5] P. A. Krug, T. D. Stephens, G. Dhosi, G. Yoffe, F. Ouellette, and P. C. Hill, *Electron. Lett.*, vol. 31, p. 1091, 1995.
- [6] W. H. Loh, R. I. Laming, N. Robinson, A. Cavaciuti, F. Vaninetti, C. J. Anderson, M. N. Zervas, and M. J. Cole, *IEEE Photon. Technol. Lett.*, vol. 8, p. 944, 1996.
- [7] F. Ouellette, *Appl. Opt.*, vol. 29, p. 4826, 1990.
- [8] B. J. Eggleton, T. Stephens, P. A. Krug, G. Dhosi, Z. Brodzeli, and F. Ouellette, *Electron. Lett.*, vol. 32, p. 1610, 1996.

- [9] N. M. Litchinitser and D. B. Patterson, "Analysis of fiber Bragg gratings for dispersion compensation in reflective and transmissive geometries," *J. Lightwave Technol.*, this issue, pp. 1323–1328.
- [10] G. P. Agrawal, *Nonlinear Fiber Optics*. New York: Academic, 1995.
- [11] P. St. J. Russel, *J. Mod. Opt.*, vol. 38, p. 1599, 1991.
- [12] J. E. Sipe, L. Poladian, and M. de Sterke, *J. Opt. Soc. Amer. A*, vol. 11, p. 1307, 1994.
- [13] B. J. Eggleton, R. E. Slusher, C. M. de Sterke, P. A. Krug, and J. E. Sipe, *Phys. Rev. Lett.*, vol. 76, p. 1627, 1996.
- [14] B. J. Eggleton, C. M. de Sterke, and R. E. Slusher, *Opt. Lett.*, vol. 21, p. 1223, 1996.
- [15] D. Marcuse, *Appl. Opt.*, vol. 19, p. 1653, 1980.
- [16] ———, *Appl. Opt.*, vol. 20, p. 3573, 1981.
- [17] S. A. Akhmanov, V. A. Vysloukh, and A. S. Chirkin, *Optics of Femtosecond Laser Pulses*. New York: AIP, 1992.
- [18] B. Malo, S. Theriault, D. C. Johnson, F. Bilodeau, J. Albert, and K. O. Hill, *Electron. Lett.*, vol. 31, p. 223, 1995.
- [19] M. Yamada and K. Sakuda, *Appl. Opt.*, vol. 26, p. 3474, 1987.
- [20] V. Mizrahi *et al.*, *Appl. Phys. Lett.*, vol. 63, p. 1727, 1993.
- [21] D. Anderson and M. J. Lisak, *Phys. Rev. A*, vol. 35, p. 184, 1987.
- [22] G. P. Agrawal and S. Radic, *IEEE Photon. Technol. Lett.*, vol. 6, p. 995, 1994.
- [23] V. Mizrahi, T. Erdogan, D. J. DiGiovanni, P. J. Lemaire, W. M. MacDonald, S. G. Kosinski, S. Cabot, and J. E. Sipe, *Electron. Lett.*, vol. 30, p. 780, 1994.
- [24] T. A. Strasser, P. J. Chandonnet, J. DeMarco, C. E. Soccolich, J. R. Pedrazzani, D. J. DiGiovanni, M. J. Andrejco, and D. S. Shenk, in *Proc. OFC'96*, 1996, postdeadline paper, PD8.
- [25] B. J. Eggleton, P. A. Krug, L. Poladian, and F. Ouellette, *Electron. Lett.*, vol. 30, p. 1620, 1994.

Natalia M. Litchinitser was born in Moscow, Russia, on May 8, 1970. She received the M.S. degree in physics from Moscow State University in 1993. She is currently pursuing the Ph.D. degree in electrical engineering.

While pursuing the M.S. degree, she was working on the effect of the stimulated Raman scattering on ultrashort pulse propagation in optical fibers. In 1994, she joined the Department of Electrical and Computer Engineering at Illinois Institute of Technology as a graduate student. Her primary research interests are in the areas of fiber and nonlinear optics. She is particularly interested in linear and nonlinear properties of fiber gratings, and dispersion compensation techniques.

Ms. Litchinitser is a student member of the Optical Society of America.



Benjamin J. Eggleton received the Bachelors degree with honors in physics from the University of Sydney, Sydney, Australia, in 1992, and the Ph.D. degree from the School of Physics at the University of Sydney and the Australian Cooperative Research Centre, Sydney, Australia, in 1996. His doctoral research focused on linear and nonlinear effects in fiber Bragg gratings.

In 1996, he joined the Department of Optical Physics at Bell Laboratories, Lucent Technologies, Murray Hill, NJ. His research interests include nonlinear optics, fiber gratings, all-optical switches, and soliton propagation.

David B. Patterson (M'93) was born in Greenfield, IA, on June 13, 1962. He received the B.S. degree in physics from Iowa State University, Ames, in 1984, and the M.S. and Ph.D. degrees in applied physics from Stanford University, Stanford, CA, in 1988 and 1990, respectively.

After working as a Research Associate at Stanford University, he joined the Electrical and Computer Engineering Department at the Illinois Institute of Technology, Chicago, in 1991 as an Assistant Professor. His research interests include acousto-optic fiber modulators, grating-based dispersion compensators, silica integrated optics, quantum cryptography, and coupled-mode interactions in fiber/planar waveguide systems.

Dr. Patterson is a member of the OSA.